Int. J. Electrochem. Sci., 9 **(2014)** 2254 - 2265

International Journal of ELECTROCHEMICAL SCIENCE
www.electrochemsci.org

Effect of Corrosion Products Formed and Flow Rate Over the Surface of Steels API 5L X-52 and X-70 on the Rate of Corrosion in Brine Added with Kerosene and H_2S

A. Cervantes-Tobón, M. Díaz-Cruz[*], *J. L. González-Velázquez, J.G. Godínez-Salcedo.*

Instituto Politécnico Nacional, Departamento de Ingeniería Metalúrgica, Laboratorios Pesados de Metalurgia UPALM, Col. Zacatenco, Del. G. A. Madero, 07738, México, D.F.
[*]E-mail: maenc_2000@yahoo.com.mx, mdiazc@ipn.mx

Received: 25 November 2013 / *Accepted:* 24 January 2014 / *Published:* 2 March 2014

This paper studies the effect of corrosion products formed and the rate of flow on the surface of two API steels on the corrosion rate in a brine added with kerosene and H_2S. Corrosion products formed over the surface have been characterized using Scanning Electron Microscopy (SEM), X-ray Diffraction (XRD) and Linear Polarization techniques. XRD and EDS analysis showed that the corrosion products are mainly composed of a mixture of oxides (maghemite, hematite, magnetite), sulfides (mackinawite, troilite, markasite, smithite) and one sulfate (mikasaite). Across SEM micrographs the corrosion products formed are very similar, covering most of the steels surface. Linear Polarization results confirm a good behavior on the rate corrosion for both steels in a range of flow rate at 4000 to 5500 rpm but the API 5L-X70 was the best behavior in the range of 4000 to the end of the test at 6500 rpm due the presence showing a greater amount of sulfur compared to the oxides thus resulting more efficient with respect to the rate of corrosion. The protective function with corrosion products on the surface of the API 5L-X-70 steel turns out to be much better compared to the other.

Keywords: Corrosion products, API 5L X-52, API 5L X-70, Acid sour media, Corrosion.

1. INTRODUCTION

In the oil and gas industries, the presence of hydrogen sulfide (H_2S) in the transported fluids causes severe corrosion problems on the steel pipelines [1]. API 5L-X52 and X70 steels are used as pipeline material in México and other countries, in natural gas, hydrocarbons and crude oil transport in the petroleum industry. However, they are susceptible to severe degradation by hydrogen sulfide (H_2S) which is nearly always present in both crude oil and natural gas, in alkaline and acid media [2-4]. The H_2S corrosion begins with the dissolution of H_2S gas in the liquid phase to form various reactive species such as hydrogen sulfide, hydrosulfide ions, sulfide ions and H + ions participating in electron

transfer in metal interface [5-7]. These are the cathodic reactions. The anodic reaction is the dissolution of Fe to form Fe^{++}. Electrochemical reactions (cathodic and anodic) in metallic surface yield corrosion products.

It has been reported that depending on the corrosion products (mainly non-stoichiometric compounds) formed on the steel in sour media can be protective or non-protective against the corrosion. Many authors propose that the first corrosion product formed on the surface of steel is the ferrous sulfide (FeS) phase, known as mackinawite [8] as a result of a solid state reaction on the surface of the corroding steel [9,10]. Mackinawite films can be extremely thin, but are characterized by the presence of others sulfides. Mackinawite (tetragonal, $FeS_{(1-x)}$) [11,12] and some stoichiometric compounds such as troilite (hexagonal FeS) [10,13] and amorphous ferrous sulfide (FeS) [14,15]. These corrosion products are weakly adherent and porous [16,17] controlled by iron dissolution and atomic hydrogen diffusion [17,18].

The present work aims at investigating the effect of the composition, morphology, and protective characteristics of the corrosion products on the deterioration behavior of API 5L-X52 and X70 pipeline steels in an acid sour solution (brine with kerosene and H_2S) by means of rotating cylindrical electrode (RCE), Scanning Electron Microscopy (SEM), X-ray diffraction (XRD) and Electrochemical technique (Potentiodynamic Polarization Resistance).

2. EXPERIMENTAL PROCEDURE

2.1. Test Environment.

The test solution was a brine prepared according to NACE standard 1D-196 with 106.5789 g/l NaCl, 4.4773 g/l $CaCl_2$ $2H_2O$, 2.061 g/l $MgCl_2$ $6H_2O$, 10% of kerosene and 1387.2 ppm of hydrogen sulfide (H_2S) were added. The pH was 3.89 and the temperature of the solution of 60ºC. The test solution was deaerated with nitrogen gas for a period of 30 minutes according to the ASTM G59-97 (Reapproved 2003) [19], to remove dissolved oxygen.

2.2. Experimental set up.

A double bottom cell made of Pyrex glass heated with hot water was used. Cylindrical tests specimens were cut off from actual pipes of 11 mm or more in thickness along the longitudinal direction. The total area exposed of the working electrode was 3.5 cm^2 for both static and dynamic tests. The reference electrode was saturated calomel electrode, and two auxiliary electrodes of sintered graphite rods were used. Before each experiment the working electrode was polished with grade 600 silicon carbide paper, cleaned with deionized water and degreased with acetone. All electrochemical tests were performed on clean recently prepared samples and fresh solutions.

2.3. Rotating cylindrical electrode (RCE).

The RCE was a computer controlled type, made by Radiometer Analytical, type EDI 10000 connected to a Potentiostat/Galvanostat. The working electrode rotational speeds used in this study were varied from 0 to 6500 rpm, with increments of 500 rpm.

2.4. Corrosion rate measurements.

A "Standard Test Method for Conducting Potentiodynamic Polarization Resistance Measurements" (ASTM G59-97 (Reapproved 2003)) was applied by means of the commercial software POWER SUIT of Princeton Applied Research by using a Potentiostat/Galvanostat Princeton Applied Research model 263A (over the range of ± 20 mV). The polarization curves were obtained at a rate of 0.166 mV per second. The corrosion rate was obtained as a function of flow rate for the steels used in brine added with 10% of kerosene in presence of H_2S at 60°C. To make the results reliable three readings were taken for each flow velocity range employed, allowing the system to stabilize for 5 minutes before running the test and retake the reading of both the potential and the corrosion rate for each of the steel used in the investigation.

2.5. Characterization of corrosion products by SEM.

The surface morphology and composition of the corrosion products formed on electrode surface was characterized and analyzed using a scanning electron microscopy (SEM) Jeol JSM 6300 operated at 20 kV, 220 μA and with a work distance of 39 mm and the coupled EDS.

2.5.1 Physical characterization by XRD

X-ray diffraction (XRD) was used to determine the iron phases on API 5L-X52 and X70 steels, with a scanned range from 20° to 90° and a step width of 0.02°, using a D8 Focus Bruker diffractometer with Cu Kα radiation. Further, analyses of XRD spectra were carried out using the CreaFit 2.2 DRXWin program.

3. RESULTS AND DISCUSSION

3.1. Chemical analysis

Chemical composition of the steels was obtained by means of a technique of atomic emission spectroscopy spark. The chemical compositions (wt.%) obtained for the steels employed here are shown in Table 1.

Table 1. Chemical composition of the API 5L X-52 and X-70 steels (wt%).

Steel	C	Mn	Si	P	S	Cr	Cu	Ni	Fe
API 5L X-52	0.111	0.955	0.175	0.005	0.022	0.037	0.293	0.013	98.3
API 5L X-70	0.240	1.081	0.284	0.019	0.021	0.156	0.185	0.088	97.8

3.2 Microestructure and grain size

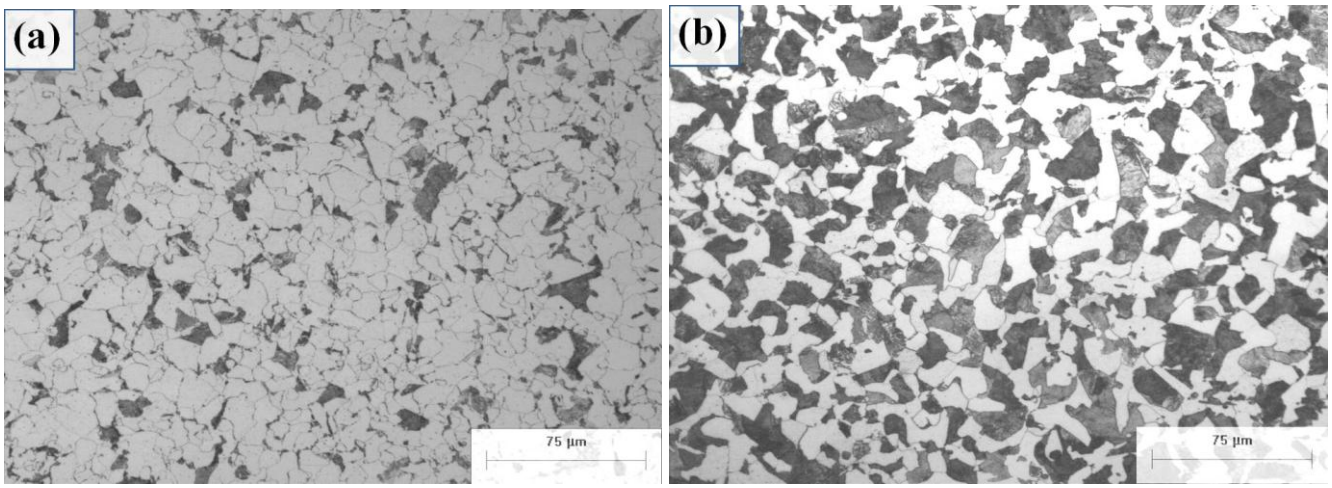

Figure 1. Micrographs of the microestructure of (a) API 5L X-52 and (b) API 5L X-70 steels.

Figure 1 shows the microstructure of the steels; in both cases it can be seen the presence of pearlite (dark phase) in a ferritic matrix (light phase). This is in agreement with similar microestructure obtained by others [20-22].

Table 2. Quantifying phases present for steels used in the present investigation along the longitudinal section.

Steel	% Ferrite	% Pearlite	ASTM Grain
API 5L X-52	86.64	13.35	8
API 5L X-70	70.51	29.48	10

For API 5L X-52 the percentage of pearlite according to Table 2 is 13.35% and 86.64% ferrite, in the case of API 5L X-70 has 29.48% pearlite and 70.51% of ferrite. With respect to the grain size (Table 2), the API 5L X-52 has a value of 8 and this is a larger grain with respect to the API 5L X-70 obtaining a value of 10 according to ASTM.

3.3 Linear polarization studies

3.3.1 Corrosion potential

Figure 2 shows the results of the corrosion potential (corrosion tendency) of the studied steels as a function of flow rate at 60 ° C in brine added with kerosene and H_2S. These results shows that the corrosion tendency is greater for the API 5L X-70, in this case the highest activity indicates corrosion products begin to form and evolve uniformly throughout the flow velocity range employed therefore it is not further seen a considerable increase in the tendency to corrosion due to the corrosion potential does not increased significantly, so it could be assumed that the corrosion products formed are more stable and uniform surface API 5L X-70.

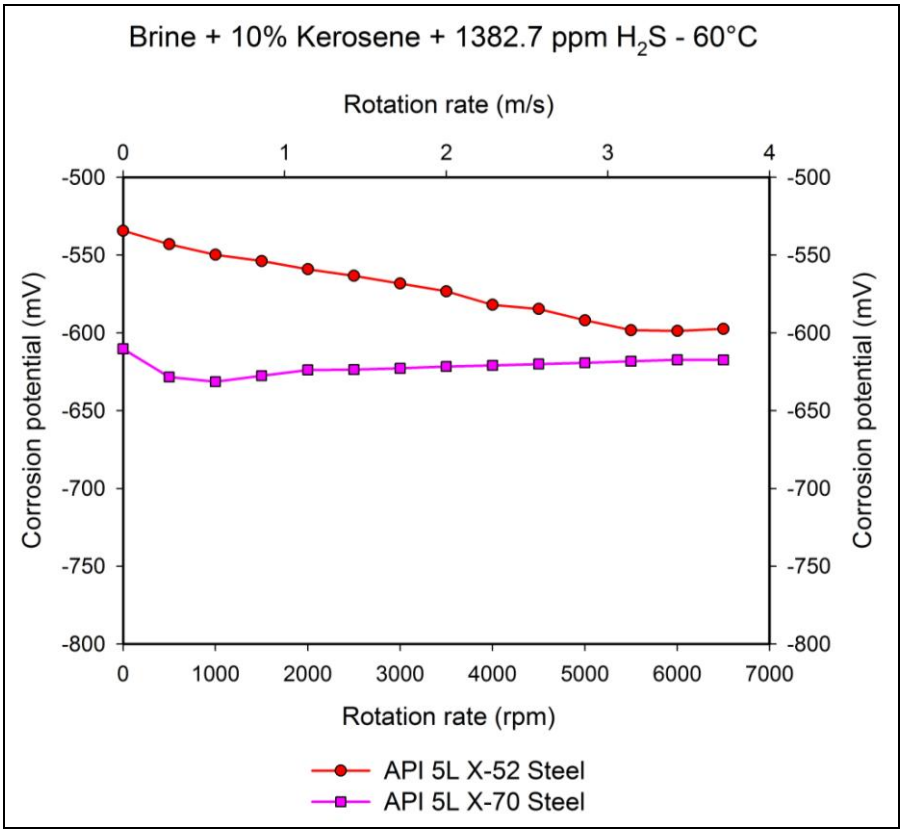

Figure 2. Corrosion potential (corrosion tendency) as a function of the flow rate for the API 5L X-52 and API 5L X-70 steel in brine added with kerosene in presence of H_2S at 60°C.

In the case of API 5L X-52 starts a less active corrosion potential and is increased continuously which we may indicate a steady growth of corrosion products which it would in turn indicate that likely there is also a greater amount of those on the surface of the steel. In both cases the corrosion potential became more positive for the API 5L X-52 is from -534.363 to -597.438 mV_{SCE} and for the API 5L X-70 is from -610.305 to -617.435 mV_{SCE}. In general, there are two causes of a positive shift of the corrosion potential; either the cathodic process on metal surface is promoted, or the anodic process is restrained [23].

3.3.2 Comparison of corrosion rates as a function of flow rates for steels API 5L X-52 and API 5L X-70 in presence of H_2S at 60°C

In figure 3 the results for the rate of corrosion of steel API 5L X-52 and API 5L X-70 in a medium added with brine kerosene and H_2S at 60 ° C, are compared to observe which has the best behavior with respect to corrosion. From these results it was observed that for both steels from the beginning corrosion rate is increased with increasing flow rate (this variation by the dependence of the corrosion rate on the flow velocity is generally attributed to a change by the corrosion mechanism [24]) up to a rotation speed of 3500 rpm, from there (4000 rpm) both steels show similar behavior to maintain a corrosion rate almost invariable up to 5,500 rpm, and is the API 5L X-70 which maintains this behavior to the end of the test (6500 rpm), thus suggesting that the corrosion products formed on the surface are more stable (there is not detachment from the same) and makes the corrosion rate remains almost constant in this range, the API 5L X-52 between 6000 and 6500 rpm shows an increase in the corrosion rate which indicates that there was a detachment of corrosion products formed due to the same action of the flow (inducing movement to the fluid, the wall shear stresses diminish the thickness of this layer [25], which lead to an increase of the corrosion rate), so these may not be as stable or have a good adherence as the other steel.

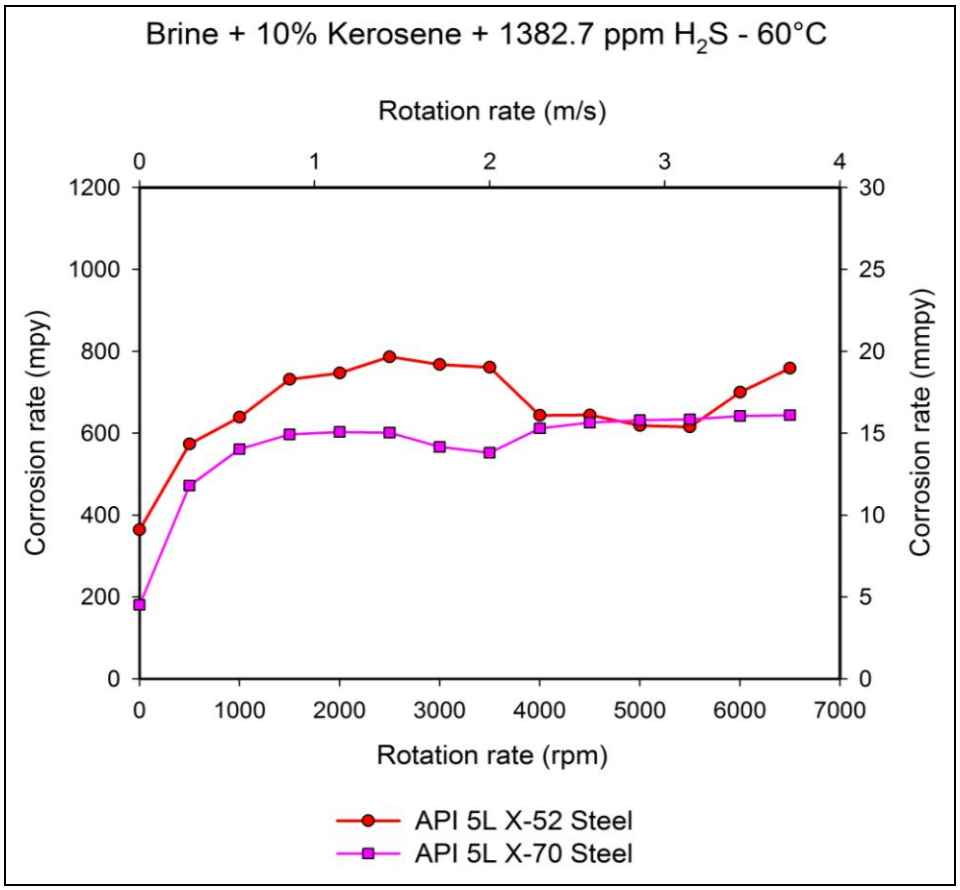

Figure 3. Corrosion rate comparison as a function of the flow rate for the API 5L X-52 and API 5L X-70 steel in brine added with kerosene in presence of H_2S at 60°C.

From the above it was observed that the API 5L X-70 has a better performance in terms of corrosion rate, the better performance attributed to its more uniform formation of corrosion products (oxides, sulfides and one sulfate) and also according to their chemical composition (Table 2) has a higher content of chromium, copper and nickel whose elements that together achieve significantly further decrease the corrosion rate as suggested by Y.S. Choi et al [26].

3.4 SEM and EDS surface characterization

3.4.1 SEM surface characterization

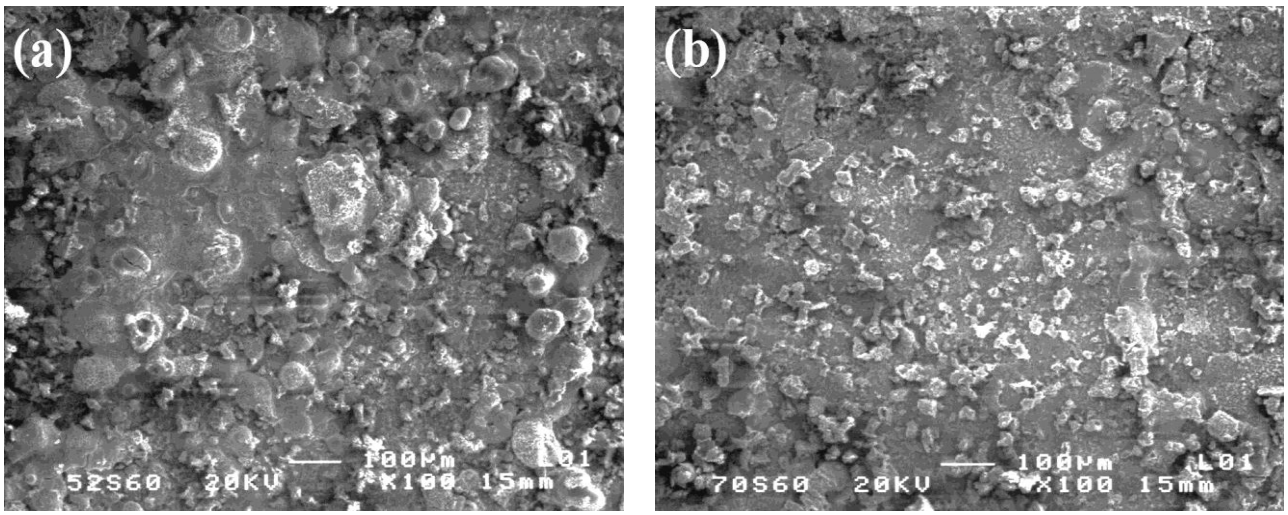

Figure 4. SEM images obtained after the formation of corrosion products on the (a) API 5L X-52 and (b) API 5L X-70 steel surface.

Corrosive deposits from steel formed in solution are mainly composed of insoluble products, undissolved constituents and trace amounts of alloying elements. They are formed various oxides and sulfides as a result of the corrosion process undergone by the metal under certain conditions or the type of medium used. Figures 4 (a) and (b) are SEM micrographs of the corrosion products formed on surfaces of the steels API 5L X-52 and X-70 at 100X magnification. In both cases a layer of amorphous corrosion products on the surface generalized being visibly most abundant and porous for API 5L X-52.

3.4.2 EDS surface characterization

Figure 5 EDS shows the measurement of (a) API 5L X-52 and (b) API 5L X-70 steel in brine added with kerosene and H_2S at 60°C primarily shows that the mainly identified elements are C, O, Fe and traced amount of Na, Ca, Mn, Si. Elements Mn and Si were from steel substrate and Na, Ca precipitated from the brine. These elements on the surface indicating the presence of the protective

FeO, Fe_2O_3, Fe_3O_4 or some sulfides as mackinawite (FeS_{1-x}),film formation (corrosion products) as reported in the literature [27-29].

It is known that H_2S contributes to the corrosion and formation of iron sulfide film. This film is formed almost instantaneously at the moment that the H_2S is added into the solution (brine) and has a black color; mackinawite is the first corrosion product formed at the iron/steel surface and usually forms as a precursor to other types of sulfides. The mackinawite film formed at the steel surface is nonadherent and cracks easily as report Shoesmith et al [30].

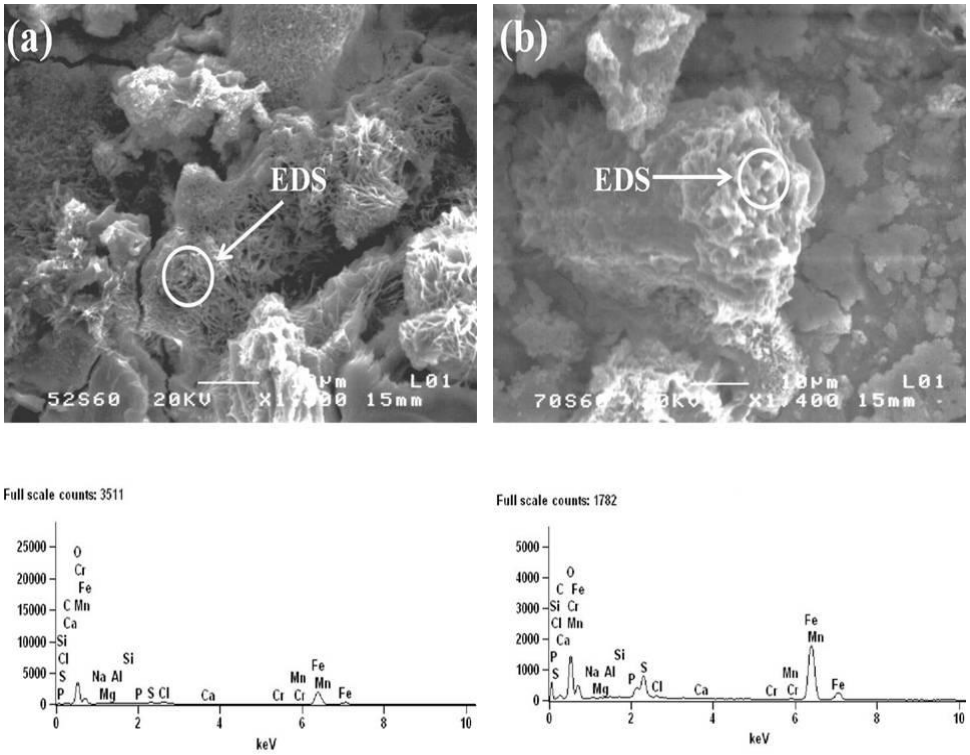

Figure 5. SEM micrographs and EDS microanalysis obtained for (a) API 5L X-52 and (b) API 5L X-70 steel surface.

Table 3. Chemical composition (wt%) of corrosion scale on API 5L X-52 and API 5L X-70 steel surface.

Elements (wt%)	(a) API 5L X-52	(b) API 5L X-70
C	10.77	11.61
O	42.25	26.39
Na	0.64	0.43
Si	0.17	0.17
S	1.69	4.06
Cl	2.13	0.80
Ca	0.08	0.00
Cr	0.00	0.01
Mn	0.14	0.45
Fe	42.10	55.93

Table 3 shows that for the API 5L X-52 corrosion products consist of a 42.10 wt% iron, 42.10% oxygen and 1.69 wt% sulfur, so it is a mixture of oxides with sulfides, for API 5L X-70 has a 55.93% wt of iron, 26.39% oxygen and 4.06 wt% wt sulfur, which be observed you will have a mixture of oxides with sulfides but in this case there will be more sulfides than oxides. In API 5L X-52 predominate over sulfide oxides for having a stronger presence of oxygen. In both cases, they show the presence of some trace elements such as Mn, Si, Ca and Cr corresponding to the steel surface and elements such as Mg, Na and Cl they could precipitate in the same brine used as a corrosive medium.

3.4.3 XRD characterization of corrosion products

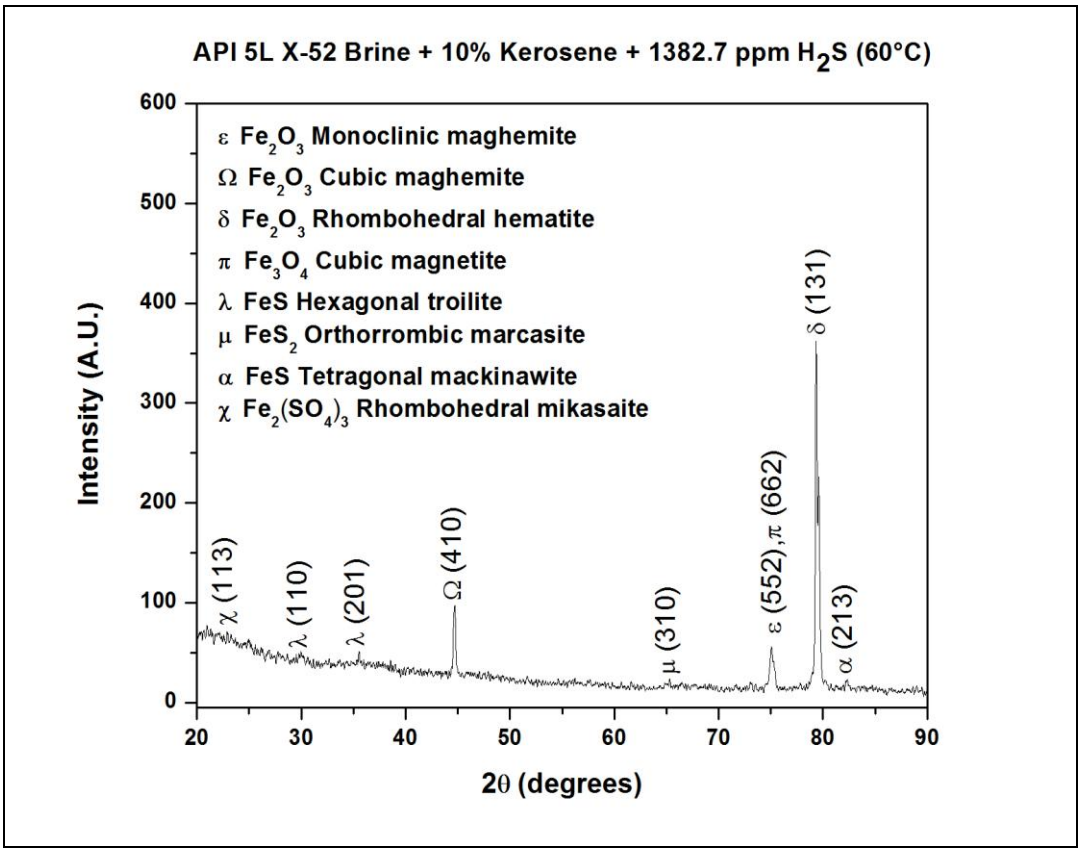

Figure 6. X-ray diffraction analysis (XRD) of corrosion products in API 5L X-52 steel surface in brine added with kerosene and H_2S at 60°C.

The study by X-ray diffraction of the corrosion products formed is revealed by Figures 6 and 7 for both steels, API 5L X-52 and X-70 is formed with a mixture of oxides and sulfurs as report of similar form A. Hernández et al [31], but also in this case sulfate is formed known as mikasaite ($Fe_2(SO_4)_3$ rhombohedral), which certainly influences the behavior of the corrosion rate and should be studied in more detail to know for certain that the effect on the corrosion rate.

The dissolved Fe^{2+} from the substrate (steel) formed iron oxides and the sulfate in this case the rhombohedral mikasaite. Sun Ah Park et al [32] report recently the presence of this compound, in this work the $Fe_2(SO_4)_3$ is a protective layer on carbon steel surfaces.

Both steels are mainly formed oxides hematite (rhombohedral), maghemite (monoclinic and cubic) and magnetite (cubic) and besides sulphides mackinawite (tetragonal) form sulfides other species as are troilite (hexagonal), the smithite and marcasite (orthorrombic). Mackinawite is a common mineral composed of tetragonal crystals, whereas troilite is hexagonal and both are consider protective layers. The different crystal structures of iron sulfides formed in H_2S containing corrosive media were describe in detail by D. Rickard et al [33]. The crystal structures or the corrosion product film significantly vary [34]. The differences of the crystal structures of iron sulfide are due to the corrosive medium differences [35]. The presence of some oxides as Fe_2O_3 and Fe_3O_4 [36], partially protects the steel surfaces from further dissolutions and leads in turn to the appearance of a passive region on the behavior of the corrosion rate as seen in some region of the graph in the figure 3 (4000 to 5000 rpm). The intensity of the peaks detected in the case of API 5L X-52 are more intense which indicates that there is a higher amount of the corrosion products formed on the surface. Therefore both steel corrosion products are acting as a protective film against the corrosion process being in the API 5L X-70 more homogeneous, stable for having more sulfides than oxides.

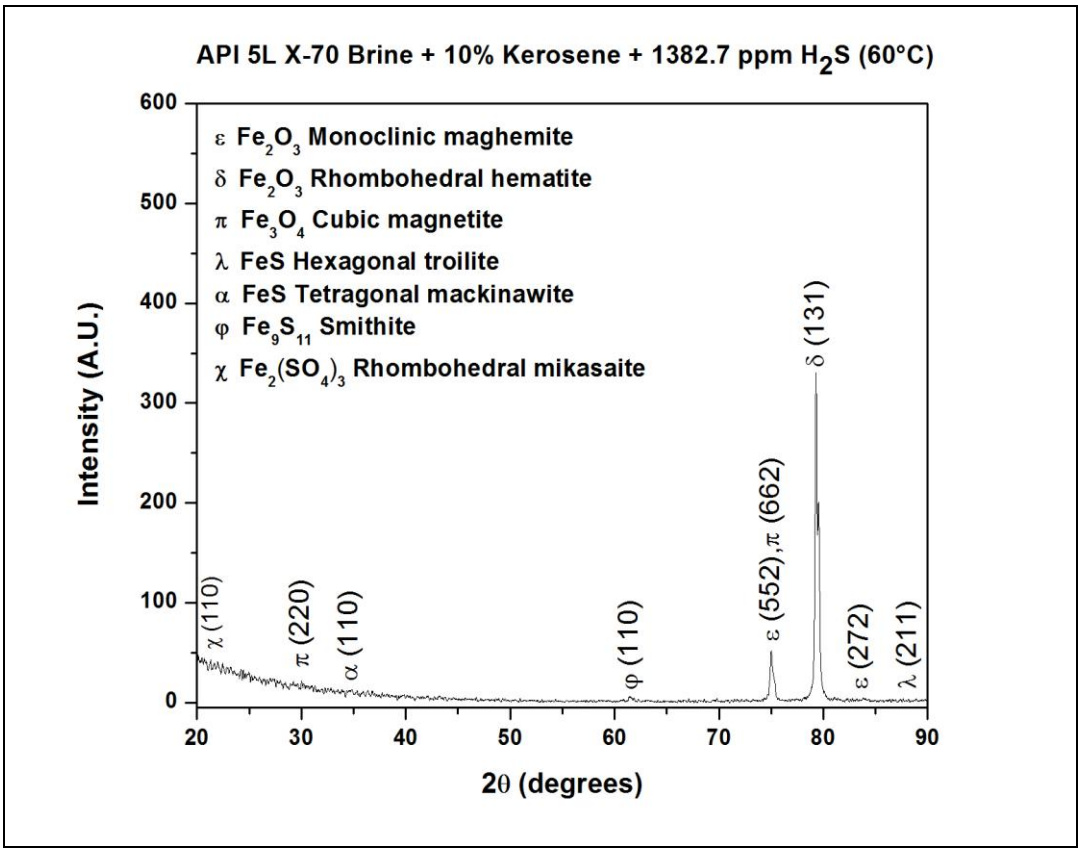

Figure 7. X-ray diffraction analysis (XRD) of corrosion products in API 5L X-70 steel surface in brine added with kerosene and H_2S at 60°C.

For API 5L X-52, although it forms a greater quantity of corrosion products are mostly oxides (less sulfides) which appear to be less adherent and suffer some detachment by the action of flow to rise the corrosion rate again, accordingly.

4. CONCLUSIONS

Characterization studies carried out by SEM showed that the corrosion products formed on the surface of each of the steels which are composed of a mixture of oxides, sulfides and a sulfate.

The API 5L X-70 steel showed the best behavior with respect to the corrosion rate because it has a lower corrosion rate compared to API 5L X-52 steel, in this case the flow rate does not have any significant effect on the formation of corrosion products, due to its corrosion products are more stable and uniform in surface although are at a lower amount as could it be seen, the greater presence of sulfides (hexagonal troilite, tetragonal mackinawite and smithite) and one sulfate (rhombohedral mikasaite) helps the better protection work as oxides (monoclinic and cubic maghemite, rhombohedral hematite and cubic magnetite) protective modifying properties as observed in the API 5L-X52 steel where there is an increased presence of these and serve as a partially protective barrier but are not as efficient as in the case of the other steel.

The best performance that has the API 5L-X70 steel with respect to the corrosion rate is also due to the presence of a greater amount of chromium, copper and nickel which together help to better performance with respect to corrosion as suggested some authors.

A lower amount of corrosion products formed is caused by a smaller amount of ferrite in the API 5L-X70 steel which is the anodic phase where they may form these corrosion products.

The present study provides a comparative study of two steels regarding the corrosion rate and the effect of corrosion products that form on the surface since normally the most research study only one steel.

ACKNOWLEDGEMENTS
The authors are also greatful for the financial support to the group of Pipeline Integrity Analysis (GAID-IPN) and corrosion laboratory for the technical support during the experimental tests, CONACYT and SIP-IPN.

References

1. M. E. Olvera-Martínez, J. Mendoza-Flores, *Mater. and Corros*., 62 (2012).1.
2. J. L. Crolet, M. R. Bonis, *Corros*., 56 (2000) 167.
3. M. Elboujdani, V. S. Sastri, R. W. Revie, *Corros*., 50 (1994) 636.
4. M. A. Lucio-García, J. G. González-Rodríguez, M. Casales, L. Martínez, J. G. Chacón-Nava, M. A. Neri-Flores, A. Martínez-Villafañe, *Corros. Sci*., 51 (2009) 2009.
5. E. C. Greco, W. B Wright, *Corrosion*, 18 (1963) 119-124.
6. J. B. Sardisco, R. E. Pitts, *Corrosion*, 21 (1965) 245-253.
7. R. N. Tuttle, R. D. Kane, A Compilation of Classic Papers, NACE, Houston, Texas (1981).
8. F. H. Meyer, O. L. Riggs, R. L McGlasson, J. D. Sudbury, *Corrosion*, 14 (1958) 69.
9. S. N. Smith, E. J. Wright, Corrosion/94, Paper no. 011 (Houston, TX: NACE International, 1994).
10. D. W. Shoesmith, P. M. Taylor, M. G. Bayley, D. G. Owen, *J. Electrochem. Sci. Technol*. 127 (1980) 1007.
11. L. J. Yan, L. Niu, H. C. Lin, W. T. Wu, S. Z. Liu, *Corros. Sci*., 41 (1999) 2305.
12. Z. F. Yin, W. Z. zhao, Z. Q. Bai, Y. R. feng, W. J. Zhou, *Electrochim Acta* 53 (2008) 3690.
13. J. B. Sardisco, W. B. Wright, E. C. Greco, *Corrosion*, 19 (1963) 353.
14. H. Vedage, T. A. Ramanarayanan, J. D. Mundford, S. N. Smith, *Corrosion*, 49 (1993) 114.

15. H. Castañeda, E. Sosa, M. A. Espinosa-Medina, *Corros. Sci*., 51 (2009) 799.
16. E. Sosa, R. Cabrera-Sierra, I. García, M. T. Oropeza, I. González, *Corros. Sci*., 44 (2002) 1515.
17. R. Cabrera-Sierra, E. Sosa, M. T. Oropeza, I. González, *Electrochim. Acta*, 47 (2002) 214.
18. S. Nesic, K. L. J. Lee, *Electrochim. Acta*, 47 (2002) 2149.
19. ASTM G59-97 (Reapproved 2003)"Standard Test Method for Conducting Potentiodynamic Polarization Resistance Measurements" (Houston TX: NACE, 2003).
20. R. Dong, I. Sun, Z. Liu, X. Wang and Q. Liu, *Journal of Iron and Steel Research International*, 15 (2008) 71
21. D. Clover, B. Kinsella, B. Pejcic and R. De Marco, *Journal of Applied Electrochemestry*, 35 (2005) 139.
22. C.W. Du, X.G. Li, P. Liang, Z.Y. Liu, G.F. Jia and Y.F. Cheng, *Journal of Materials Engineering and Performance*, 18 (2009) 216.
23. J. Liu, Y. Lin, X. Yong, X. Li, *Corrosion*, 61 (2005) 1061.
24. U. Lotz, *Corrosion*/90, Paper no. 27 (Houston TX:NACE International, 1990).
25. D. Silverman, *Corrosion*/90, Paper no. 13 (Houston TX:NACE International, 1990)
26. Y.S. Choi, J.J. Shim, J.G. Kim, *ournal. of Alloys and Compunds*, 391 (2005) 162.
27. P.R. Rhodes, *Corros. Sci.*, 57 (2001) 923.
28. I. Hamada and K. Yamauchi, *Metall. Mater. Trans. A Phys. Metall. Mater. Sci.*, 5 (2010) 56.
29. CH. Ren, D. Liu, Z. Bai and T. Li, *Mater. Chem. Phys*., 93 (2005) 305.
30. D.W. Shoesmith, P. taylor, M.G. Bailey, D.G. Owen, *J. Electrochem. Soc.*, 127 (1980) 5.
31. A. Hernández-Espejel, M.A. Dominguez-Crespo, R. Cabrera-Sierra, C. Rodriguez-Meneses, E.M Arce-Estrada, *Corros. Sci*., 52 (2010) 2258.
32. S.A. Park, W.S. Ji, J.G. Kim, *Int. J. Electrochem. Sci*., 8 (2013) 7498.
33. D. Rickard and G. Luther, *Chem. Rev.*, 107 (2007) 514.
34. D. Rickard and J. Morse, *Mar. Chem*., 97 (2005) 141.
35. E. Díaz, J. Gonzalez-Rodriguez, R. Sandoval-Jabalera, S. Serna, B. Campillo, M. Neri_flores, C. Gaona-Tiburcio and A. Martínez-Villafane, *Int. J. Electrochem. Sci*., 5 (2010) 1821.
36. El-Sayed M. Sherif, Abdulhakim A. Almajid, Khalil Abdelrazek Khalil, Harri Junaedi and F.H. Latief, *Int. J. Electrochem. Sci*., 8 (2013) 9360.